Identification of potential sites for aquifer storage and recovery (ASR) in coastal areas using ASR performance estimation methods

Koen G. Zuurbier · Mark Bakker · Willem Jan Zaadnoordijk · Pieter J. Stuyfzand

Abstract Performance of freshwater aquifer storage and recovery (ASR) systems in brackish or saline aquifers is negatively affected by lateral flow, density effects, and/or dispersive mixing, causing ambient groundwater to enter ASR wells during recovery. Two recently published ASR performance estimation methods are applied in a Dutch coastal area, characterized by brackish-to-saline groundwater and locally high lateral-flow velocities. ASR performance of existing systems in the study area show good agreement with the predicted performance using the two methods, provided that local vertical anisotropy ratios are limited (<3). Deviations between actual and predicted ASR performance may originate from simplifications in the conceptual model and uncertainties in the hydrogeological and hydrochemical input. As the estimation methods prove suitable to predict ASR performance, feasibility maps are generated for different scales of ASR to identify favorable ASR sites. Successful small-to-medium-scale ASR varies spatially in the study area, emphasizing the relevance of reliable a priori spatial mapping.

Keywords Aquifer storage and recovery · Recovery efficiency · Coastal aquifers · Freshwater management · The Netherlands

Received: 27 November 2012 / Accepted: 19 May 2013
Published online: 19 June 2013

K. G. Zuurbier (✉) · W. J. Zaadnoordijk · P. J. Stuyfzand
KWR Watercycle Research Institute,
Groningenhaven 7, 3433 PE, Nieuwegein, The Netherlands
e-mail: koen.zuurbier@kwrwater.nl

K. G. Zuurbier · P. J. Stuyfzand
Critical Zone Hydrology Group, Department of Earth Sciences,
VU University Amsterdam,
De Boelelaan 1085, 1081 HV, Amsterdam, The Netherlands

M. Bakker · W. J. Zaadnoordijk
Water Resources Section, Faculty of Civil Engineering
and Geosciences, Delft University of Technology,
Stevinweg 1, 2628 CN, Delft, The Netherlands

Introduction

Aquifer storage and recovery (ASR) is defined as "the storage of water in a suitable aquifer through a well during times when water is available, and the recovery of water from the same well during times when it is needed" (Pyne 2005). It may be a successful technique for storage and recovery of both potable and irrigation water (Dillon 2005; Dillon, et al. 2006; Maliva et al. 2006; Pyne 2005; Vacher et al. 2006). ASR may have many purposes, including supply during peak demands, seasonal or diurnal storage, and purification. The fraction of the injected water that can be recovered with a certain accepted quality is called the recovery efficiency (RE), which is a performance indicator of ASR. The RE can be reduced in coastal areas due to density differences between the injected freshwater and ambient brackish or saline groundwater. In such cases, freshwater floats upwards through the aquifer (buoyancy effect), while denser saline water is recovered by lower parts of the well (Esmail and Kimbler 1967; Merritt 1986; Ward et al. 2007). The loss of recoverable freshwater may be further increased by lateral groundwater flow, causing injected freshwater to move outside the capture zone of the ASR well, where it cannot be recovered (Bear and Jacobs 1965).

It is important to predict the ASR-performance before large investments are made, considering all the relevant factors. Ward et al. (2007, 2008, 2009) showed that not only salinity, but also aquifer thickness, hydraulic conductivity, hydraulic gradient, aquifer anisotropy, and hydrodynamic dispersion need consideration. Furthermore, operational parameters such as pumping rates, injection volume and injection-, storage-, and recovery durations need to be considered when potential ASR-performance is analyzed. ASR performance estimation therefore traditionally requires extensive and expensive data collection and advanced numerical modeling to reduce uncertainties in important aquifer parameters (Misut and Voss 2007; Pavelic et al. 2002; Pyne 2005; Ward et al. 2007, 2008, 2009). Ward et al. (2009) and Bakker (2010) recently proposed two relatively simple methods to predict ASR performance by a fully penetrating well. Potential performance of ASR can be predicted using these methods, without rigorous numerical modeling, taking into account common hydrogeological data and operational parameters. However, there is little field verification and application of these theoretical performance estimation methods known to date in geologically varying brackish and saline aquifers due to a scarcity of monitored ASR systems.

The objective of this report is to assess the predicted ASR performance by Ward et al. (2009) and Bakker (2010) through comparison with the measured performance of existing ASR sites in a coastal area. The applicability and drawbacks of both methods are analyzed and maps are generated of hydrologically potential ASR sites in the study area. Maps of predicted spatial ASR performance provide important information on the potential use of ASR as a freshwater management strategy in the study area.

Study area

Westland-Oostland greenhouse area

The combined Westland and Oostland area in The Netherlands (Fig. 1) is an intensive greenhouse horticultural area facing irrigation-water-related issues. The salinity requirements of the irrigation water in this area (generally measured using electrical conductivity, EC) are exceptionally strict; drinking water is already too saline for many of the crops and flowers cultivated. Low salinity allows greenhouse owners to reuse drained water from artificial substrates multiple times, without reaching critical sodium concentrations. Fresh irrigation water supply is realized primarily by storing low EC rainwater from greenhouse roofs in basins or tanks, complemented by the use of surface water in periods of low salinity and by desalination of brackish groundwater (Stuyfzand and Raat 2010).

A mismatch in precipitation and water demand creates a large winter freshwater surplus (Fig. 2), which is discharged to sea, as only a small part can be stored in basins or tanks. Surface water is generally unsuitable as a source of freshwater during summer droughts, as they are fed by brackish seepage water (de Louw et al. 2010). Fresh surface water can be brought in from major rivers, but the inlets suffer increasingly from salinization caused by seawater intrusion during summer droughts, which is exacerbated by sea-level rise (Barends et al. 1995; Kooi 2000; Kwadijk et al. 2010; Oude Essink et al. 2010; Post 2003; Schothorst 1977). Summer droughts are predicted to become more intense and prolonged, whereas wintertime precipitation is expected to increase 3.5–7 % (Intergovernmental Panel on Climate Change, IPCC 2007; van den Hurk et al. 2007). Freshwater availability for irrigation during summer will likely be reduced due to the changing temporal precipitation distribution in combination with a predicted rise in temperature. Up to now, desalination by reverse osmosis is the only proven technology to ensure freshwater supply. Major disadvantages of this technique are the high energy consumption, the required maintenance, and especially the disposal of leftover concentrate. Discharge of this concentrate to sewage systems or surface waters is not allowed and a ban on its disposal in deeper saline aquifers is being prepared.

A more sustainable use of the precipitation surplus collected by greenhouse roofs will improve freshwater availability in the area. ASR is a cost-effective, readily applicable technique to store large water volumes, without the need for large surface areas. In the study area, ASR has been applied on a small scale since the 1980s in the upper, relatively shallow aquifer (10–50 m below surface level,

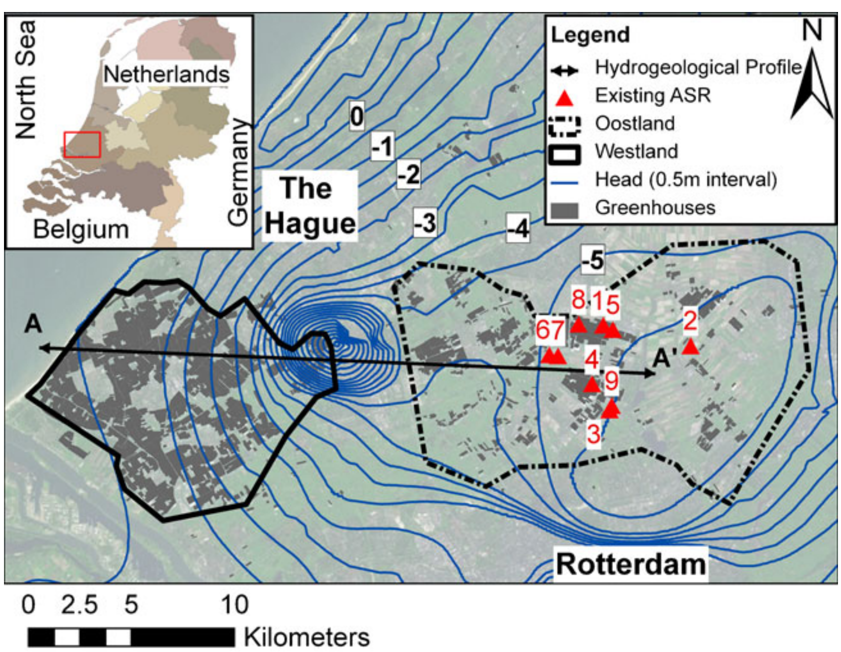

Fig. 1 Locations of the Westland and Oostland greenhouse areas near *The Hague* and *Rotterdam* and hydraulic heads in Aquifer I from the 'Data and information system of the Dutch subsurface' (TNO-NITG 2011). For the hydrogeological profile, see Fig. 3. Studied ASR systems are coded by no. *1–9*

 DOI 10.1007/s10040-013-1003-2

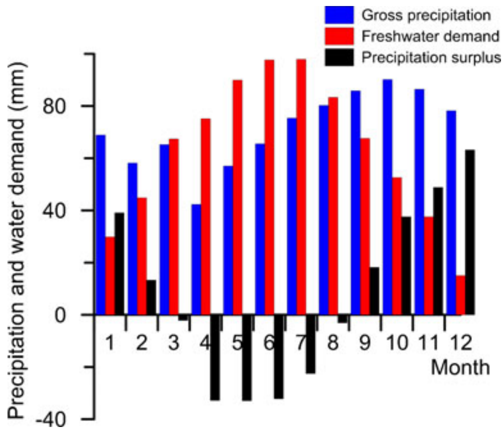

Fig. 2 Mean gross monthly precipitation (1980–2010) near the study area (weather station Rotterdam, Royal Netherlands Meteorological Institute), estimated monthly water demand of intensive horticulture, and resulting estimate of available water for ASR (Paalman et al. 2012)

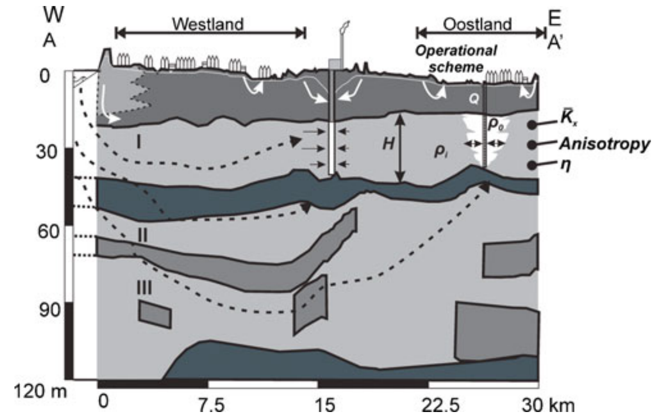

Fig. 3 Cross-section of the study area based on the REGIS II.1 hydrogeological model from the 'Data and information system of the Dutch subsurface' (TNO-NITG 2011). Flow lines interpreted from regional hydrological system analysis (Negenman et al. 1996). Important factors for ASR performance are highlighted for example ASR system in the Oostland area (not to scale). *I*, *II* and *III* are aquifers. H is the aquifer thickness, $\overline{K}_x$ is the average horizontal conductivity, η is the effective porosity, ρ_{i} is the ambient groundwater density and ρ_0 is the injection water density. Q is the pumping rate during ASR operation

mbsl; Fig. 3), which is the thinnest and least saline aquifer found in the area.

Hydrogeological setting

Unconsolidated Pleistocene and Holocene fluvial and marine deposits are found in the upper ~120 m of the study area (Fig. 3, TNO-NITG 2011). These middle-to-late Pleistocene clays, sands, and gravels were deposited by former Rhine-Meuse fluvial systems and during marine transgressions (Busschers et al. 2005). The transition to groundwater with chloride concentrations >1,000 mg/L is found at a depth of only a few meters in Westland (Post 2003), and somewhat deeper in Oostland (−5 to −40 mbsl). Regional groundwater flow is controlled by the North Sea in the west, the lower drainage level of the deep polders in Oostland, and a large industrial groundwater extraction in the middle areas which results in high flow velocities in its vicinity (Figs. 1 and 3). Aquifer I is also exploited for brackish water to supply desalinated greenhouse irrigation water; the concentrate is injected in Aquifers II and III (Fig. 3).

ASR performance estimation

ASR performance has been measured at nine existing ASR systems. First, the measured performance is compared to the predicted performance using two recently presented ASR estimation methods. Next, a spatial ASR feasibility analysis is performed and ASR feasibility maps are generated.

Detailed ASR operational parameters have not been recorded. General ASR operational parameters are estimated from the mean monthly precipitation record (1980–2010) registered near the Westland-Oostland area and from the estimated mean monthly water demand of the local horticulture by Paalman et al. (2012). Total mean yearly gross precipitation is 853 mm, while the mean yearly water demand is 679 mm. The estimated ASR operational parameters and water availability and demand (both in m^3/m^2/year) are presented in Table 1.

Performance of existing ASR systems, Oostland

The total injected and recovered volumes of nine systems outfitted with water meters (for locations, see Fig. 1) were inventoried at the end of the summer recovery period in August 2011 (Table 2). The studied systems were at the end of cycle 2, 4, 5, 6, or 9. The injected and recovered volumes of multiple cycles are used to calculate the total RE during the lifespan of each system. This total RE is considered the minimum total RE for the ASR lifespan, as it is unknown whether freshwater was recovered until a maximum EC was reached, or whether recovery was terminated because water demand was met. Based on the maximum EC, the allowed mixing fraction is calculated. The mixing fraction f (−) is defined as the proportion of injected water in the recovered water as a function of time during recovery (Pavelic et al. 2002; Ward et al. 2007):

$$f = \frac{C_i - C(t)}{C_i - C_0} \quad (1)$$

Table 1 General ASR operational parameters and mean water availability and demand in the study area

Period	Duration (days)	General water availability (+) or demand (−) (m^3/m^2)
Injection	150	+ 0.2
Storage	30	0
Recovery	120	– 0.12
Idle	65	0

 DOI 10.1007/s10040-013-1003-2

Table 2 Age, allowed mixing fraction, injected and recovered volumes/rates, and the total recovery efficiency (*RE*) of measured ASR systems in the Oostland area

ASR system (No., Fig. 1)	Age (years)	Allowed mixing fraction *f* (−)	Yearly injection volume (×1000 m^3)	Injection rate (m^3/day)	Yearly recovery volume (×1000 m^3)	Recovery rate (m^3/day)	Total RE (%)
1	6.0	0.56	28.3	188	17.1	143	61
2	8.8	0.72	35.3	235	29.2	243	83
3	4.0	0.79	46.0	307	23.4	195	51
4	1.9	0.83	22.4	150	10.2	85	45
5	5.7	0.66	44.4	296	26.4	220	59
6	4.0	0.77	24.6	164	14.8	123	60
7	4.4	0.41	16.9	113	9.2	77	55
8	5.8	0.51	86.7	578	54.4	453	63
9	4.8	0.87	47.5	317	30.0	250	63

where C_i is the concentration of the ambient groundwater, $C(t)$ is the concentration at time t in the recovery phase and C_0 is the concentration of the injection water. The mixing factor varies per system due to differences in background salinity of the aquifer and allowed maximum salinity of the recovered water. If a relatively low mixing ratio is allowed, measured ASR performance can be higher than predicted.

The mean pumping rate for each system during injection and recovery is based on the general durations of the injection and recovery period (Table 1), the registered injected and recovered volumes, and the age of each system. In case a system was installed during an injection period, injected volumes are distributed over fewer months of operation.

ASR performance estimation methods

Method of Ward et al. (2009)

Ward et al. (2009) proposed four dimensionless ratios for the qualitative prediction of ASR performance: a technical viability ratio, focusing on the lateral drift during storage, a dispersivity ratio for the effect of dispersive mixing, a mixed convection ratio to characterize the density effects during injection and recovery, and a storage tilt ratio to determine the significance of density-driven flow during storage. All parameters equally contribute to the overall indicator of ASR performance.

The technical viability ratio (R_{TV}) is defined as:

$$R_{TV} = \left| \frac{\overline{K}_x \cdot I \cdot t_s}{\eta \cdot x_{i,u}} \right| \tag{2}$$

where $\overline{K}_x$ is the average horizontal hydraulic conductivity (L/T), I is the hydraulic gradient (−), t_s is the duration of storage (T), η is the porosity (−) and $x_{i,u}$ is the location of the injected freshwater in the centre of the aquifer in the upstream direction at the end of the injection period (L).

The dispersivity ratio (R_{disp}) is defined as:

$$R_{disp} = \frac{\beta_L}{x_{i,u}} \tag{3}$$

where β_L is the longitudinal dispersivity (L).

The mixed convection ratio (M) is defined as:

$$M = \frac{\overline{K}_z \alpha}{\left| \frac{Q}{2\pi H \eta x_{i,u}} \right| - \left| \frac{\overline{K}_x I}{\eta} \right|} \tag{4}$$

where $\overline{K}_z$ is the average vertical hydraulic conductivity (L/T), α is the density difference ratio (−), Q is the pumping rate (L^3/T) and H is the aquifer thickness (L).

The storage tilt ratio (R_{ST}) is defined as:

$$R_{ST} = \frac{\overline{K}_z \alpha H t_s}{\eta (x_{i,u})^2} \tag{5}$$

The overall indicator R_{ASR} is defined as:

$$R_{ASR} = R_{TV} + R_{disp} + M + R_{ST} \tag{6}$$

The density difference ratio (α) is defined as:

$$\alpha = \frac{\rho_i - \rho_0}{\rho_0} \tag{7}$$

where ρ_i is the concentration of the ambient groundwater (M/L^3) and ρ_0 is the density of the injected water (M/L^3). Based on modeling results, Ward et al. (2009) concluded for one ASR-cycle that: (1) when R_{ASR} is smaller than 0.1, the mixing ratio *f* is 1 at the beginning of recovery and at least 0.8 after half of the injected volume is recovered, and ~0.4 at a RE of 100 %, (2) the interval $0.1 < R_{ASR} < 10$ is a transitional range in which the dimensionless ratios cannot predict success or failure, and (3) undesirable sites/regimes are marked by an $R_{ASR} \geq 10$, meaning *f* is around 0 at the start of recovery. This method provides a qualitative prediction of the performance of the first ASR cycle only; the potential RE is not predicted.

DOI 10.1007/s10040-013-1003-2

R_{TV}, R_{ST} and R_{disp} are calculated following Ward et al. (2009). For calculation of M, Ward et al. (2009) assumed equal pumping rates during the injection and recovery phases. The recovery pumping rate is significantly smaller (33 %) than the injection rate for the systems considered here. In this study therefore, $x_{i,u}$ is calculated following Ward et al. (2009) using the injection rate, while M is calculated using the recovery rate. As a consequence, it is possible to obtain negative values for R_{ASR} when the background groundwater velocity exceeds the velocity caused by pumping during recovery at $x_{i,u}$. In such cases, counteraction of free convection at the fringe of the freshwater body by pumping is limited, density effects are dominant, and M is set to 10.

Method of Bakker (2010)

Bakker (2010) proposed a screening tool considering loss of freshwater by buoyancy effects only. Using interfaces and a new solution for radial Dupuit interface flow, it was shown that the RE (defined as the part of the injected water recovered until the toe of the freshwater–saltwater interface reaches the well screen) is dependent on the dimensionless parameter D:

$$D = \frac{Q}{\overline{K}_x \alpha H^2} \tag{8}$$

For each combination of relative lengths of injection, storage and recovery periods, the RE can be calculated for each value of D and for each cycle. Groundwater mixing is not taken into account. Hence, this screening tool results in an upper limit of the RE and is intended to assess whether further study of ASR performance is worthwhile. Bakker (2010) does not take into account plume distortion by lateral flow. In this study, zones where plume distortion is expected are identified based on the dimensionless time parameter $\bar{t}$ defined as:

$$\bar{t} = \frac{2\pi t_{inj} H}{\eta Q}\left(\overline{K}_x I\right)^2 \tag{9}$$

where t_{inj} (T) is the duration of the injection period.

When $\bar{t}$ is<0.1, lateral flow can be neglected (Ceric and Haitjema 2005; Ward et al. 2009). The RE was calculated for each D for the injection, storage, and recovery durations of Table 1, and a 25 % higher pumping rate during recovery in order to get the maximum RE limited by the interface only and not by the duration of recovery. The total estimated RE was calculated for each system, using the injection rate and number of cycles of each system, and compared with the measured total RE.

ASR feasibility in Westland-Oostland

Use of ArcGIS

Spatial maps are generated of the required injection rate to achieve successful ASR, indicated by a RE of 60 % in cycle 5 (Bakker 2010) or a R_{ASR} of 0.1 (Ward et al. 2009). The durations of injection, storage, and recovery periods are shown in Table 1, and the recovery rate is 75 % of the injection rate. The Model Builder of ArcGIS (version 9.3) is used to perform all calculation steps on a 100 × 100 m grid (resolution of the hydrogeological input) to predict the required injection rate for each cell. Ten iterations are performed after an initial injection rate of 50 m^3/day using the method by Ward et al. (2009), adapting the injection rate based on the outcome of R_{ASR} in each step to achieve R_{ASR}=0.1. For the method of Bakker (2010), a RE of 60 % in cycle 5 is achieved when D is higher than 14.3, and the required injection rate is calculated in each cell for this D. Subsequently, the dimensionless $\bar{t}$ corresponding to this pumping rate is calculated to exclude areas with plume distortion from the dataset.

Hydrogeological input

Top elevation, bottom elevation, transmissivities, and standard deviations of K_x of the hydrogeological units of the Holocene cover, Aquifer I, and Aquitard I were taken from the Regional Geohydrological Information System (REGIS) of the 'Data and information system of the Dutch subsurface' (TNO-NITG 2011). The thickness of Aquifer I (target aquifer) was derived by summation of the hydrogeological units consisting of sand below the Holocene cover, but above the first regional aquitard (Formation of Peize-Waalre, unit Waalre-Clay1). The few cells in which Aquitard I was absent and Aquifer I and II formed one (thick) aquifer were removed from the dataset. Transmissivities of the hydrogeological units were summed in order to obtain the total transmissivity of the aquifer. A mean horizontal hydraulic conductivity ($\overline{K}_x$) was computed from this aquifer transmissivity and the aquifer thickness. Ward et al. (2008) demonstrated that a homogeneous anisotropy ratio (K_x over K_z) can be used to account for stratification of the aquifer and that higher anisotropy ratios improve ASR performance. As data on these anisotropy ratios are often scarce, a sensitivity analysis is performed using anisotropy ratios of 1 (isotropic) and 3 (anisotropic) in the estimation performance by Ward et al. (2009). A mean porosity (η) of 0.35 was used (Meinardi 1994). The hydraulic gradient was calculated using the interpolated head data from the 'Data and information system of the Dutch subsurface' of Aquifer I on April 28, 1995 (TNO-NITG 2011, see Fig. 1). A longitudinal dispersivity (β_L) of 0.1 m was used.

Groundwater quality data (chloride concentrations)

Chloride concentrations were used to represent salinity and to estimate groundwater densities. A three-dimensional (3-D) interpolation of the chloride concentrations was

 DOI 10.1007/s10040-013-1003-2

developed by Oude Essink et al. (2010) based on vertical electrical soundings, geo-electrical well logs, and chloride concentration measurements at observation wells. The interpolated data were stored in a 250×250 m raster file with a vertical resolution of 5 m. Chloride concentrations at the centre of Aquifer I were estimated using the top and bottom elevations of the aquifer. Those chloride concentrations were converted to groundwater densities using (Oude Essink et al. 2010):

$$\rho(C_{cl}) = \rho_0 + 0.00134 \cdot C_{cl} \tag{10}$$

where ρ is the density of the water (kg/m^3), C_{cl} is the chloride concentration (mg/l) and ρ_0 is the density of freshwater (1,000 kg/m^3). The effect of temperature variations of the injection water on water density was neglected, as this can be presumed limited for the range of temperature differences during the infiltration period (Ma and Zheng 2010).

Results

Comparison of the predicted and measured ASR performance

The ASR performance indicator R_{ASR} is plotted versus the total RE from measurements for an isotropic hydraulic conductivity (Fig. 4a) and for an anisotropy factor of 3 (Fig. 4b). The parameter R_{ASR} indicates uncertain performance for all systems (i.e., R_{ASR} >0.1) when isotropy is assumed. R_{ASR} is <0.5 (isotropic) and <0.13 (anisotropic; ratio=3) for all systems. ASR system 3 has a R_{ASR} of 0.08 (anisotropic) to 0.23 (isotropic), and a total RE of 51 % in 4 years. It may be expected that this system will recover ~60 % of the injected water in cycle 5. Based on measured RE, successful ASR systems are therefore marked by R_{ASR}<0.23 (isotropic), or R_{ASR}<0.08 in the anisotropic case. The results indicate that the qualitative method proposed by Ward et al. (2009) is at least reasonable in the study area, as R_{ASR} is generally low when ASR performance is high. It is confirmed that for R_{ASR} <0.1, successful ASR can be expected. Overestimating the anisotropy may result in an unrealistic increase in the predicted performance; R_{ASR} is around or below 0.1 for all systems, with only limited uncertainty.

The measured total RE is compared to the predicted total RE with the method of Bakker (2010) in Fig. 5. At three systems, the measured RE is lower than the predicted RE. Six systems performed better than predicted, even though the estimation method should give an upper limit. For five of these systems, the measured RE is within the uncertainty range based on one standard deviation for $\overline{K}_x$. One ASR system performed significantly better than predicted (83 vs. 35 %), whereas one system recovered significantly less than predicted (63 vs. 78 %). In the latter case, this can be due to a low water demand and therefore limited recovery. The other system, performing better than predicted, was installed in a thick, relatively anistropic aquifer with a relatively fine-grained base, which may have delayed salinization at the bottom of the ASR well. The predicted RE is generally in line with the measured RE. The results suggest that the screening tool by Bakker (2010) can indeed be used to predict RE in the study area.

Spatial mapping of potential ASR sites

Maps are developed showing the predicted ASR performance for the entire study area. The predicted ASR performance increases with injection rate (or indirectly the ASR scale, as the injection time remains constant), which is therefore used as an indicator for spatial ASR suitability. The required injection rate for successful

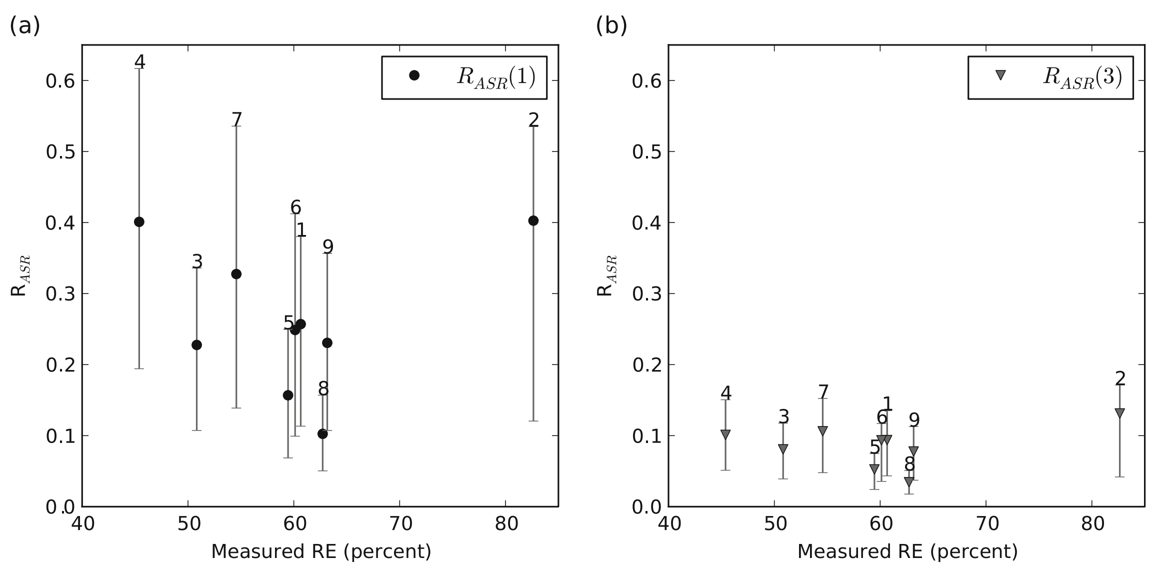

Fig. 4 Measured RE versus predicted ASR performance. Relation with R_{ASR} is shown for the **a** isotropic and **b** anisotropic case (anisotropy ratio=3). *Error bars* represent the results for one standard deviation in uncertainty for the hydraulic conductivity input

 DOI 10.1007/s10040-013-1003-2

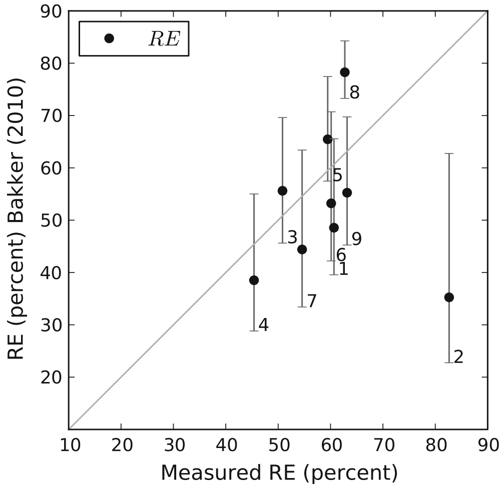

Fig. 5 Predicted total RE Bakker (2010) versus the measured total RE. *Error bars* represent the results for one standard deviation in uncertainty for the hydraulic conductivity input. The *continuous line* indicates predicted RE = measured RE

ASR using Ward et al. (2009) varies up to 4 orders of magnitude (Fig. 6), highlighting the large variation in potential ASR performance in the study area. For an isotropic case, successful ASR is predicted in the Oostland for an injection rate of 500–5,000 m^3/day, or 50–2,500 m^3/day for the anisotropic case. In the Westland, a high mean injection rate of more than 10,000 m^3/day is required for the isotropic case and about 5,000 m^3/day for the anisotropic case.

The mean required injection rate for successful ASR is ~300 m^3/day in the Oostland area according to Bakker (2010), whereas in the Westland area a mean injection rate of ~800 m^3/day is required. The latter confirms the limited suitability of this particular area for small-to-medium-scale ASR application, although projections are better than predicted by Ward et al. (2009). More suitable ASR sites are predicted in general with this method, compared to the method by Ward et al. (2009). Spatial mapping using Bakker (2010) also illustrates the large variations in aquifer suitability for freshwater ASR, with minimum injection rates increasing from 50 to more than 1,000 m^3/day within a distance of 2 km.

Discussion

Comparison of the measured and predicted ASR performance

The ASR performance estimation presented by Ward et al. (2009) cannot be correlated directly to a RE. Based on the existing systems, successful ASR sites are marked by R_{ASR} <0.23 for the isotropic case or <0.08 for an anisotropy ratio of 3. This indicates that this method is suitable for a qualitative performance analysis, and that the proposed required R_{ASR} of 0.1 for certain success is appropriate in the study area (which does not rule out successful ASR when R_{ASR} >0.1). This R_{ASR} value is therefore small enough to ensure ASR success, even though the different ratios are lumped with an equal contribution. The anisotropy ratio should not be overestimated in the area, as a high ASR performance is predicted at all systems with limited uncertainty for an anisotropy ratio of 3, whereas in reality more differentiation is found. In this comparison, two out of nine systems performed outside the 65 % confidence interval (based on the uncertainty in $\overline{K}_x$). One system performed significantly worse, which may be explained by a limited water demand, and therefore limited recovery. Another system performed much better than predicted, but is installed in a relatively thick, potentially anisotropic aquifer. Six systems performed better than predicted by Bakker (2010), which should overestimate RE.

Although the predicted RE is in line with the measured RE, deviations are observed and potential explanations can be addressed. The performance estimation tools are for instance based on confined aquifers having an impermeable top and base; thus, not considering semi-confined aquifers. It is known that the lower confining clay layer of the target aquifer locally has a limited resistance (TNO-NITG 2011), making the ASR-well partially penetrating a thick aquifer. In this study, the performance estimation is limited to areas where the upper aquifer was underlain by a clay layer in the REGIS hydrogeological model, but no further deviations based on the resistance of those aquitards and vertical head gradients are made. Seepage is therefore neglected and may cause early salinization at the bottom of the ASR well. This study can be used to identify unsuitable parts of the target aquifer for future ASR with a specific injection rate, independent of seepage. Furthermore, the potential RE is predicted using Bakker (2010) neglecting aquifer vertical anisotropy, for instance by stratification of isotropic units in the target aquifer with a different K, which might underestimate the potential RE due to an anisotropy ratio larger than 1 (Ward et al. 2008). The method by Ward et al. (2009) takes into account this (potential) vertical anisotropy, resulting in a significant increase in area where successful ASR is predicted for an anisotropy ratio of 3. Although a limited anisotropy ratio is presumed (<3) based on the measured and the predicted REs using Ward et al. (2009), aquifer stratification may be a cause for the underestimation of the RE at six out of nine sites by Bakker (2010). Altogether, both methods have their own advantages and disadvantages, of which the most important ones are given in Table 3. These should be taken into account in future spatial ASR feasibility studies.

Differences between predicted and measured performance for both methods can also originate from the available hydogeological and hydrochemical data. The regional geological model, which is based on local data (bore logs, pumping tests) has its uncertainties, since interpretation and interpolation of bore log data is required to cover large areas. The same holds for the background salinity distribution. The datasets incorporate the relative regional variations in aquifer thickness, hydraulic conductivity and salinity, which can be considered sufficient for an initial ASR performance prediction and mapping of potential ASR sites. The latter is confirmed by the agreement between the predicted and measured ASR performance.

DOI 10.1007/s10040-013-1003-2

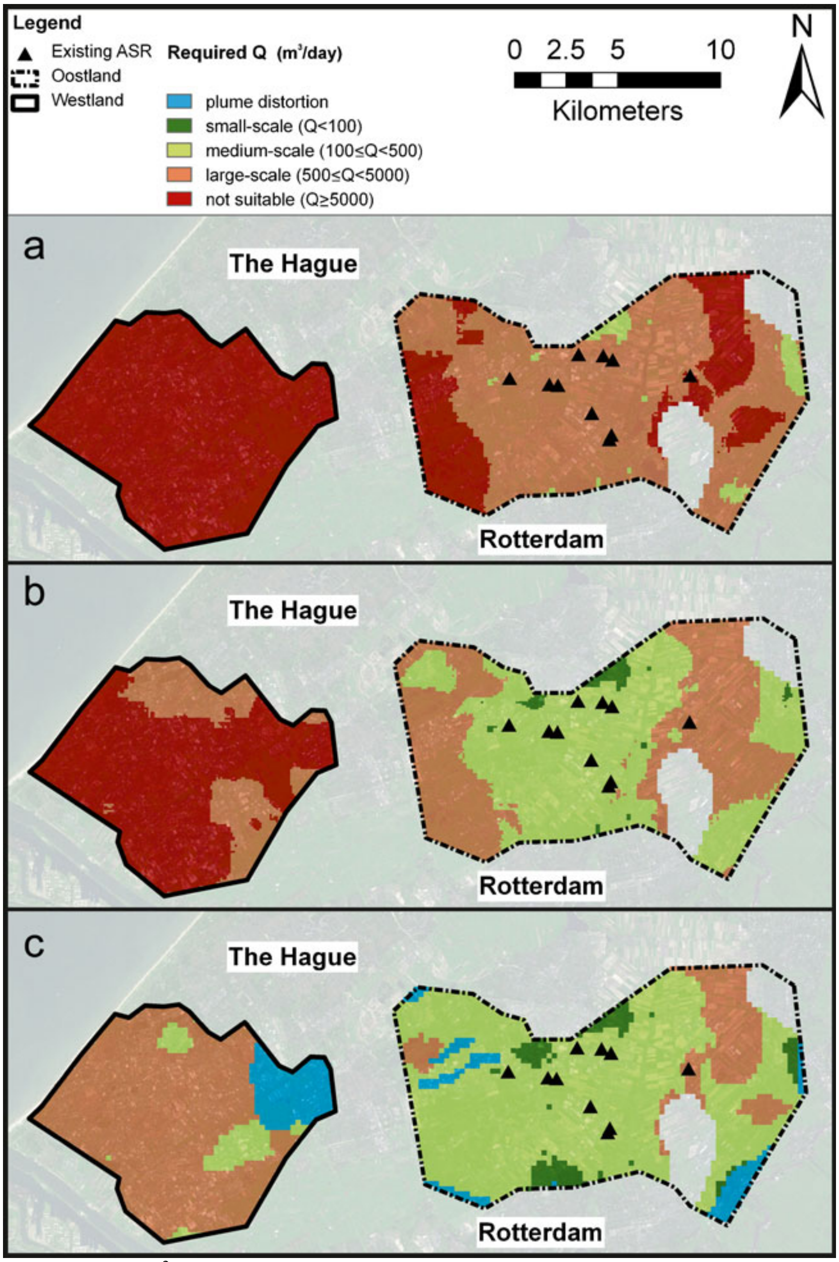

Fig. 6 Required winter injection rates (m^3/day) for successful ASR (R_{ASR} =0.1) predicted using Ward et al. (2009) for **a** the isotropic case and for **b** anisotropy ratio=3, and **c** predicted using Bakker (RE=60 % in cycle 5). No mapping is performed where Aquitard 1 is absent

ASR operation in the study area

In this study, general durations of injection, storage and recovery periods, and the total injected and recovered volumes of each system in multiple years of operation are used to derive the mean pumping rates for each ASR site. Yearly variations are neglected, which may affect ASR performance; this cannot be investigated further, as no data were recorded. An improved registration using (automatic) logging of (daily) injected and recovered volumes is essential for better assessment of performance.

Both ASR performance estimation methods consider fully penetrating wells. Use of multiple partially penetrating wells in a single borehole may lead to higher recovery efficiencies. Although its benefit for freshwater recovery has not been quantified to date, this ASR well type may increase the RE by enhanced injection at the aquifer base and/or recovery at the aquifer top, delaying salinization at the bottom of the ASR recovery well(s). Especially in the case of small-scale freshwater ASR and a thicker but relatively homogeneous aquifer, injected freshwater bodies have a limited radius, making flow conditions at the fringe of the injected freshwater body significantly different from fully penetrating wells, especially when the aquifer is anisotropic (Hantush 1966). The loss caused by buoyancy effects may

 DOI 10.1007/s10040-013-1003-2

Table 3 Comparison of ASR performance methods for spatial mapping

Ward et al. (2009)	Bakker (2010)
Input K_x, K_z, η, I, H, α Operational ASR parameters Fully penetrating well	Input K_x, H, α Operational ASR parameters Fully penetrating well
Lacks estimation of RE	Lacks lateral flow and mixing
Suitability for spatial mapping All factors can be calculated based on common geological data (+) Takes into account lateral flow and anisotropy (+) May overestimate minimum injection rates required for certain success (−)	Suitability for spatial mapping Easy to calculate D from common geological data (+) Direct estimation of RE (+) from D, but relation between D and RE needs to be derived first (−) Lateral flow and anisotropy are not considered (−) Predicts realistic minimum injection rates required for success (+)

therefore be partly counteracted, as demonstrated for a case with partially penetrating wells for aquifer thermal energy storage (ATES, Buscheck et al. 1983; Molz et al. 1983a, b). Although multiple partially penetrating wells are installed at existing systems, the systems studied were recovering and injecting over the full aquifer thickness, shutting off lower sections only when salinization at those well sections occurred. A limited increase in freshwater recovery is expected by this strategy, which is another explanation for the higher RE of some of the existing ASR systems, compared to their predicted RE. Although quantification of the potential increase in RE by such a well configuration and pumping scheme is a relevant research question, it is beyond the scope of this study.

ASR performance in the Westland-Oostland area

Good agreement is obtained between predicted and measured ASR performance, which justifies application of the estimation methods to generate feasibility maps for new ASR sites. Excluding the areas where plume distortion may be expected and single-well ASR performance is expected to be low (marked by $\bar{t} > 0.1$), the aquifer suitability is best quantified using Bakker (2010). As only a few ASR sites are predicted to be unsuitable due to plume distortion by lateral flow, it was shown that success of ASR in the study area mainly depends on freshwater loss by buoyancy effects.

Conventional small-scale ASR (Q<100 m^3/day) using a fully penetrating well is expected to have a poor performance in large parts of the study area. Spatial maps also show large variations over small distances, which highlight the relevance of a priori spatial mapping and site-selection. The required mean pumping rate in the more suitable Oostland area indicates that medium-scale ASR (100<Q<500 m^3/day) is potentially successful in a large part of the area. Only large-scale ASR (Q>500 m^3/day) can be successful in the Westland area, which is caused by the relatively thick and fairly saline aquifer. In this area, rainwater harvesting by a large cluster of greenhouses to feed one central ASR system may result in injection rates large enough for successful ASR.

ASR appears to be a suitable technique for freshwater supply in a large coastal study area, based upon average operational parameters. Between 1980 and 2010, annual precipitation varied between 605 and 1,150 mm in the study area, with a mean gross precipitation of 853 mm. This means that in wet years injection rates may be higher, recovery rates need to be lower and larger water volumes are stored for longer periods, and vice versa for relatively dry years. It is well known that long-term aquifer storage is less efficient, but still higher REs can be expected in the cycle following a wet year with relatively limited recovery, potentially supplying sufficient irrigation water even if the subsequent summer is extremely dry. This study does not quantify the RE under varying operational parameters.

Geochemical reactions during aquifer residence of the fresh, oxic rainwater may severely affect the quality of the stored water and is a well-known pitfall in ASR operation (e.g., Jones and Pichler 2007; Prommer and Stuyfzand 2005; Pyne 2005; Wallis et al. 2010). This study neglects geochemical changes in the injection water and focuses on hydrological feasibility only. Reactions during aquifer residence may make the recovered water unsuitable irrespective of the EC or chloride concentration. Oxidation of pyrite, a mineral present in the target aquifers in the study area (Busschers et al. 2005) may, for instance, mobilize trace elements, which can make the recovered water unsuitable for further use. Such geochemical studies are needed to determine feasible ASR sites based on the maps in Fig. 6.

Conclusions

Two recently developed ASR performance estimation tools were applied to predict ASR performance in a coastal area in the Netherlands. Comparison of predicted with measured ASR performance of systems in the study area show good agreement between measured and predicted total RE using the method of Bakker (2010). The performance factor (R_{ASR}) of Ward et al. (2009) correlates with successful ASR systems for R_{ASR} <0.23 for isotropic aquifers, and R_{ASR} <0.08 for a vertical anisotropy factor of 3. This confirms that successful ASR may be expected for R_{ASR} lower than ~0.1, provided that the anisotropy ratio is low (<3). Deviations between measured and predicted ASR performance may originate from simplifications in the conceptual model and uncertainties in

 DOI 10.1007/s10040-013-1003-2

the hydrogeological and hydrochemical input. Good agreement between measured and predicted performance justifies the use of both methods for spatial analysis of predicted ASR performance in this area. Maps were generated showing areas suitable for small-, medium-, and large-scale ASR systems. Successful small-to-medium ASR application is spatially variable in the study area, highlighting the relevance of a priori spatial mapping.

Acknowledgements This research was funded by the Knowledge for Climate research programme as part of the theme ‘Climate Proof Freshwater Supply’ of this program. We thank Dr. Gualbert Oude-Essink for providing the dataset of the chloride distribution in the study area.

References

Bakker M (2010) Radial Dupuit interface flow to assess the aquifer storage and recovery potential of saltwater aquifers. Hydrogeol J 18:107–115. doi:10.1007/s10040-009-0508-1

Barends BJ, Brouwer FJJ, Schröder FH (1995) Land subsidence, natural causes, measuring techniques, the Groningen gasfields. Balkema, Rotterdam, The Netherlands

Bear J, Jacobs M (1965) On the movement of water bodies injected into aquifers. J Hydrol 3:37–57

Buscheck TA, Doughty C, Tsang CF (1983) Prediction and analysis of a field experiment on a multilayered aquifer thermal energy storage system with strong buoyancy flow. Water Resour Res 19:1307–1315. doi:10.1029/WR019i005p01307

Busschers FS, Weerts HJT, Wallinga J, Cleveringa P, Kasse C, De Wolf H, Cohen KM (2005) Sedimentary architecture and optical dating of Middle and Late Pleistocene Rhine-Meuse deposits: fluvial response to climate change, sea-level fluctuation and glaciation. Neth J Geosci 84:25–41

Ceric A, Haitjema H (2005) On using simple time-of-travel capture zone delineation methods. Ground Water 43:408–412. doi:10.1111/j.1745-6584.2005.0035.x

de Louw PGB, Oude Essink GHP, Stuyfzand PJ, van der Zee SEATM (2010) Upward groundwater flow in boils as the dominant mechanism of salinization in deep polders, The Netherlands. J Hydrol 394:494–506. doi:10.1016/j.jhydrol.2010.10.009

Dillon P (2005) Future management of aquifer recharge. Hydrogeol J 13:313–316. doi:10.1007/s10040-004-0413-6

Dillon P, Pavelic P, Toze S, Rinck-Pfeiffer S, Martin R, Knapton A, Pidsley D (2006) Role of aquifer storage in water reuse. Desalination 188:123–134

Esmail OJ, Kimbler OK (1967) Investigation of the technical feasibility of storing fresh water in saline aquifers. Water Resour Res 3:683–695. doi:10.1029/WR003i003p00683

Hantush MS (1966) Wells in homogeneous anisotropic aquifers. Water Resour Res 2:273–279. doi:10.1029/WR002i002p00273

Intergovernmental Panel on Climate Change (IPCC) (2007) Climate Change 2007: the physical science basis In: Solomon S, Qin D, Manning M, Chen Z, Marquis M, Averyt KB, Tignor M, Miller HL (eds) Contribution of Working Group I to the Fourth Assessment Report of the IPCC, New York

Jones GW, Pichler T (2007) Relationship between pyrite stability and arsenic mobility during aquifer storage and recovery in southwest central Florida. Environ Sci Technol 41:723–730

Kooi H (2000) Land subsidence due to compaction in the coastal area of The Netherlands: the role of lateral fluid flow and constraints from well-log data. Glob Planet Change 27:207–222

Kwadijk JCJ, Haasnoot M, Mulder JPM, Hoogvliet MMC, Jeuken ABM, van der Krogt RAA, van Oostrom NGC, Schelfhout HA, van Velzen EH, van Waveren H, de Wit MJM (2010) Using adaptation tipping points to prepare for climate change and sea level rise: a case study in the Netherlands. WIRs Clim Change 1:729–740. doi:10.1002/wcc.64

Ma R, Zheng C (2010) Effects of density and viscosity in modeling heat as a groundwater tracer. Ground Water 48:380–389. doi:10.1111/j.1745-6584.2009.00660.x

Maliva RG, Guo W, Missimer TM (2006) Aquifer storage and recovery: recent hydrogeological advances and system performance. Water Environ Res 78:2428–2435

Meinardi CR (1994) Groundwater recharge and travel times in the sandy regions of the Netherlands. PhD Thesis, Vrije Universiteit, Amsterdam, The Netherlands

Merritt ML (1986) Recovering fresh water stored in saline limestone aquifers. Ground Water 24:516–529. doi:10.1111/j.1745-6584.1986.tb01031.x

Misut PE, Voss CI (2007) Freshwater–saltwater transition zone movement during aquifer storage and recovery cycles in Brooklyn and Queens, New York City, USA. J Hydrol 337:87–103

Molz FJ, Melville JG, Güven O, Parr AD (1983a) Aquifer thermal energy storage: an attempt to counter free thermal convection. Water Resour Res 19:922–930. doi:10.1029/WR019i004p00922

Molz FJ, Melville JG, Parr AD, King DA, Hopf MT (1983b) Aquifer thermal energy storage: a well doublet experiment at increased temperatures. Water Resour Res 19:149–160. doi:10.1029/WR019i001p00149

Negenman AJH, Foppen JWA, Kloosterman FH, Witte JPM, Meijden Rvd, Groen CLG (1996) Landelijke hydrologische systeemanalyse; deelrapport 3: ‘Deelgebied Noord- en Zuid-Holland ten zuiden van het Noordzeekanaal’ [National hydrologic system analysis; report 3: ‘Part of the provinces of North and South Holland, South of the Northsea Canal’, in Dutch]. IGG-TNO, Utrecht, The Netherlands

Oude Essink GHP, van Baaren ES, de Louw PGB (2010) Effects of climate change on coastal groundwater systems: a modeling study in the Netherlands. Water Resour Res 46:W00F04. doi:10.1029/2009wr008719

Paalman M, Appelman W, Creusen R, Stein N, Raterman B, Voogt W (2012) Vergroten zelfvoorzienendheid watervoorziening Glastuinbouw: Watervraag Glastuinbouw Haaglanden (deel 1) [Enlarging selfsufficient horticultural freshwater supply: greenhouse areas Haaglanden (part 1), in Dutch]. Case Haaglanden Knowledge for Climate, Utrecht, The Netherlands

Pavelic P, Dillon P, Simmons CT (2002) Lumped parameter estimation of initial recovery efficiency during ASR. In: Dillon PJ (ed) Fourth International Symposium on Artificial Recharge (ISAR4). Swerts and Zeitlinger, Adelaide, Australia, pp 285–290

Post VEA (2003) Groundwater salinization processes in the coastal area of the Netherlands due to transgressions during the Holocene. PhD Thesis, Vrije Universiteit, The Netherlands

Prommer H, Stuyfzand PJ (2005) Identification of temperature-dependent water quality changes during a deep well injection experiment in a pyritic aquifer. Environ Sci Technol 39:2200–2209

Pyne RDG (2005) Aquifer storage recovery: a guide to groundwater recharge through wells, 2nd edn. ASR Systems LLC, Gainesville, FL

Schothorst CJ (1977) Subsidence of low moor peat soils in the western Netherlands. Geoderma 17:265–291

Stuyfzand P, Raat K (2010) Benefits and hurdles of using brackish groundwater as a drinking water source in the Netherlands. Hydrogeol J 18:117–130. doi:10.1007/s10040-009-0527-y

TNO-NITG DINOloket (2011) www.dinoloket.nl. Accessed December 2011

Vacher HL, Hutchings WC, Budd DA (2006) Metaphors and models: the ASR bubble in the Floridan Aquifer. Ground Water 44:144–154. doi:10.1111/j.1745-6584.2005.00114.x

van den Hurk B, Tank AK, Lenderink G, van Ulden A, van Oldenborgh GJ, Katsman C, van den Brink H, Keller F, Bessembinder J, Burgers G, Komen G, Hazeleger W, Drijfhout S (2007) New climate change scenarios for the Netherlands. Water Sci Technol 56(4):27–33

Wallis I, Prommer H, Simmons CT, Post V, Stuyfzand PJ (2010) Evaluation of conceptual and numerical models for arsenic mobilization and attenuation during managed aquifer recharge. Environ Sci Technol 44:5035–5041. doi:10.1021/es100463q
Ward JD, Simmons CT, Dillon PJ (2007) A theoretical analysis of mixed convection in aquifer storage and recovery: how important are density effects? J Hydrol 343:169–186
Ward JD, Simmons CT, Dillon PJ (2008) Variable-density modelling of multiple-cycle aquifer storage and recovery (ASR): importance of anisotropy and layered heterogeneity in brackish aquifers. J Hydrol 356:93–105
Ward JD, Simmons CT, Dillon PJ, Pavelic P (2009) Integrated assessment of lateral flow, density effects and dispersion in aquifer storage and recovery. J Hydrol 370:83–99

DOI 10.1007/s10040-013-1003-2